BIOMATH
https://biomath.math.bas.bg/biomath/index.php/biomath
Biomath Forum
ORIGINAL ARTICLE

Parameter sensitivity analysis for CO-mediated sickle cell de-polymerization

Liping Liu[1,*], Mufeed Basti[2], Yao Messan[1], Guoqing Tang[1], Nicholas Luke[1]

[1]Department of Mathematics and Statistics,
[2]Department of Chemistry,
North Carolina Agricultural and Technical State University, USA
lliu@ncat.edu, basti@ncat.edu, yao.messan@gmail.com,
tang@ncat.edu, luke@ncat.edu

Received: February 1, 2023, Accepted: December 3, 2023, Published: March 14, 2024

Abstract: **This study investigates the impact of melting/binding rates (referred to hereafter as the parameters) over the polymers and monomers on the dynamics of carbon-monoxide-mediated sickle cell hemoglobin (HbS) de-polymerization. Two approaches, namely the traditional sensitivity analysis (TSA) and the multi-parameter sensitivity analysis (MPSA), have been developed and applied to the mathematical model system to quantify the sensitivities of polymers and monomers to the parameters. The Runge-Kutta method and the Monte-Carlo simulation are employed for the implementation of the sensitivity analyses. The TSA utilizes the traditional sensitivity functions (TSFs). The MPSA enumerates the overall effect of the model input parameters on the output by perturbing the model input parameters simultaneously within large ranges. All four concentrations (namely, de-oxy HbS monomers, CO-bound HbS monomers, de-oxy Hbs polymer and CO-bound HbS polymer) as model outputs, and all four binding/melting rates (namely, the CO binding and melting rates for polymers and monomers) as input parameters are considered in this study. The sensitivity results suggest that TSA and MPSA are essentially consistent.**

Keywords: **sickle cell, CO-mediated de-polymerization, sensitivity functions, multi-parameter sensitivity analysis**

I. Introduction

The sickle cell trait originates as a natural mutation of the hemoglobin gene. Such mutation results in replacement of glutamic acid at position 6 of the beta chain ($\beta 6$) of hemoglobin by valine. The mutation results in the aggregation, in the form of a polymer, of the sickle cell hemoglobin (HbS) when it is in the de-oxygenated state [1]. The polymerization process takes place in two stages, which are separated by a time delay [2]: 1) homogeneous polymerization where monomers join to form a polymer; 2) heterogeneous polymerization where monomers join an existing polymer. The polymers formed in the first step can melt yielding monomers if they return to the lungs quickly enough to be re-oxygenated. The polymers that do not return to the lungs in a timely manner will likely go through the second stage. The mechanisms for the homo- and heterogeneous polymerization are referred to as single and double nucleation [3].

Ferrone's work [3] focused on the growth of sickle hemoglobin (HbS) polymers or fibers. He explained that the growth of the HbS fibers follows the double nucleation mechanism, which he described as homogeneous and heterogeneous nucleation. The formation of a polymer is initiated by homogeneous nucleation in the solution phase. Local temperature and concentration of the homogenous nuclei can then increase the formation of additional polymers on the surface of an existing polymer (heterogeneous nucleation). Local temperature is very relevant to our work because we are looking at the change in the rate constant where

 *Corresponding author

Citation: Liping Liu, Mufeed Basti, Yao Messan, Guoqing Tang, Nicholas Luke, Parameter sensitivity analysis for CO-mediated sickle cell de-polymerization, Biomath 13 (2024), 2312036, https://doi.org/10.55630/j.biomath.2023.12.036

temperature is the only factor that causes the change in parameters. The surface area of heterogeneous nuclei is constantly increasing with time [3]. From the understanding of these two processes, Ferrone developed a mathematical model for the melting of the polymers (de-polymerization) on the assumption that the polymer melting is the reversal of polymerization. The model can be described by two rate equations, one for the formation of polymers and the second for the incorporation of monomers into polymers.

The kinetics of the sickle cell hemoglobin polymer melting has been studied experimentally by using the stopped flow method where the melting was monitored using light scattering [2]. The results showed that polymers melt more quickly in cells containing oxygen or carbon monoxide. Therefore, two sets of experiments were conducted to study polymer melting. The first experiment involved monitoring the rate of HbS polymer melting in a deoxygenated phosphate buffer at pH 7.1, 25°C, and in the second experiment the same buffer was saturated with carbon monoxide (CO) [2]. The author concluded that polymers melt more efficiently in presence of CO. Additionally, the authors noted that for the model to fit the experimental data, CO was assumed to bind to HbS in the polymeric and in the monomeric form [2]. In Aroutiounian's study [2], the model was rewritten as a system of two equations by including the fact that polymer only melts from the ends. Thus, the study improved Ferrone's model, which is based on a single differential equation. Further investigation of the effects of CO binding to the depolymerization of solution phase of the polymer used a nonlinear model that extended the original two-species model [2] into a model that included the four species: deoxy HbS monomers, CO-bound HbS monomers, deoxy Hbs polymer and CO-bound HbS polymer [4]. The model assumed that CO binds to both the monomeric and polymeric forms of HbS and described the dynamic interaction in each phase of the melting and their CO binding processes. Results from the analyses predicted that melting of de-oxy polymers occurs rapidly when the solution was saturated with CO. Additionally, they observed from the model equations that not all the polymers melt in the CO- binding equilibrium stage, indicating that the melting of the CO-bound polymer takes place as an equilibrium process.

Normally cell behaviors are determined by the interaction of the components in the biological system instead of the characteristics of the individuals. The impact on the system output from various parameters is usually different. In biological experiments, the impacts from different parameters are often difficult to determine as it requires the repeated experiments and the subtle measurements which may be practically impossible [5]. This, however, can be easily achieved in mathematical modeling with numerical simulations by parameter sensitivity analysis. Sensitivity analysis is the study of how the uncertainty in the model output can be attributed to different sources of uncertainty in its inputs [5,6]. This sensitivity analysis provides guidance toward the parameters that must be taken into consideration during the experimental design [7].

There have been studies concerning parameter estimation, which have led to approximation of parameters value in the nonlinear dynamic system [2, 4]. However there remains the possibility to improve the measurement of the parameter values. In this paper the importance of parameters in the extended model of melting (de-polymerization) of HbS polymers in the presence of CO is assessed.

There are many approaches to study the sensitivity of a model output with respect to the input parameter [5]. A comprehensive evaluation of various sensitivity analysis methods (including the FAST and Sobol methods) is provided in a case study on a hydrological model [8]. This study particularly focuses on a traditional sensitivity analysis (TSA) and a multi-parameter sensitivity analysis (MPSA) on the extended version of the model with four species [4]. All four concentrations as model outputs and four binding/melting rates as input parameters are considered in this study. The sensitivity analysis results from TSA and MPSA are essentially consistent.

The remainder of this paper consists of the following sections. Section 2 presents the derivation of the mathematical model equations starting from a description of the double nucleation process to the extended CO-mediated sickle cell polymer melting (de-polymerization). Then, Section 3 explains the detailed methodology of the parameter sensitivity analysis including the TSA and MPSA. Section 4 reports and discusses the obtained results from our analysis. Section 5 summarizes the conclusion of the study and provides the recommendation for future work. Lastly, Appendix includes the detailed sensitivity equations for TSA.

II. Model Equations

A. *Double Nucleation Mechanism*

Our current version of the model is an extension of the basic model proposed in [2,3]. The model developed for the HbS polymer melting is based on the observation that the HbS fiber melting is the reversal of growth.

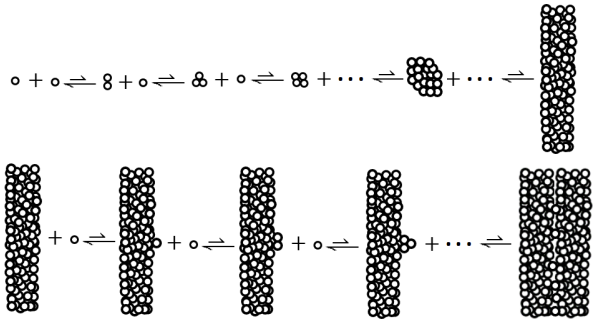

Fig. 1: The double nucleation model. Homogeneous nucleation (top) and heterogeneous nucleation (bottom) nuclei are assumed to be pieces of the infinite polymer [3].

According to [3], the growth of fiber occurs through a double nucleation process. Figure 1 depicts the process.

As it happens in the solution, homogeneous nucleation is the simple process where the monomers attach to each other to form a polymer. In heterogeneous nucleation, the monomers add onto an existing polymer to form a more complex polymer. As Fig. 1 depicts, the length of the arrows going back and forth changes in the different stages of the figure, which indicates the change in the relative rates of fibers melting or growth. In the early stages of the homogeneous nucleation phase the rate constant of melting (K_{backward}) is higher than the rate constant of growth (K_{forward}). The equilibrium stage (K_{eq}), where the rate constants of the growth and melting are the same ($K_{\text{forward}} = K_{\text{backward}}$), happens when the polymer reaches a certain size. Beyond this size, the rate of the polymer growth becomes higher than the rate of melting. The driving force for this switch in kinetics is the increase in the stability of the polymer as it exceeds the above-mentioned size. This increase in stability is due to the increasing amount of energy released as more and more monomers join the polymers which makes the polymer formation to have higher negative ΔG (meaning polymer formation becomes thermodynamically more favorable). The same cascade of events takes place in the heterogeneous nucleation phase. Again, when the size of the polymer exceeds a certain limit the formation –or growth– of the polymer becomes more favorable than the melting of the polymer. The final size of the polymer is limited by its solubility. This means once the size of the polymer –the fiber– in the heterogeneous nucleation exceeds a certain limit it becomes insoluble, or a better explanation is that the polymer stops growing when there are no more monomers to bind to it. When the size of the polymer reaches this limit it would deplete the solution from any monomers –now the concentration of the monomer to begin with is limited by its solubility at the conditions at hand (temperature, phosphate buffer concentration and the fact that the buffer is saturated with carbon monoxide).

The double nucleation model can be described by two rate equations, one for the homogeneous and the other for the heterogeneous. Since in either homogeneous or heterogeneous nucleation there is an addiction of a monomer to the nucleus, they both can be represented as (this applies to the CO bound and deoxygenated polymer) the equilibrium $P_i + (\text{monomers}) \iff P_j$. Here P_i and P_j are two forms of the polymer where the j form has one monomer more than the i form, or P_i is the homogeneous polymer and P_j is the heterogeneous polymer. The formation of the polymer is thus expressed by:

$$\frac{dC_{p,j}(t)}{dt} = k_+ C_m(t) C_{p,i}(t) - k_- C_{p,j}(t) \qquad (1)$$

and the rate of disappearance of the monomers from the solution phase into polymer is given by:

$$-\frac{dC_m(t)}{dt} = k_+ C_m(t) C_{p,i}(t) - k_- C_{p,j}(t) \qquad (2)$$

where $C_{p,i}(t)$ and $C_{p,j}(t)$ are the time-dependent concentration of polymers i and j, respectively, and $C_m(t)$ is the monomer concentration, k_+ is the concentration–independent rate constant for addition of monomers to nuclei or polymer i , and k_- is the concentration- independent rate of the dissociation of a monomer from polymer j.

B. The Simple Model with Two Equations

Briefl [9] observed that the growth is an elongation and the melting is a shortening of the HbS fiber at the ends. Thus melting of the HbS polymers can only occur at the end of the polymers. On a short time scale, the concentration of polymers P_i and P_j remains constant at a certain time. Therefore, Aroutiounian [2] sets the concentration of polymers P_i and P_j to be the same as $C_p(t)$; he replaced k_+ with $\frac{k_-}{C_s}$, where C_s is the solubility concentration of the de-oxygnated HbS polymer in the buffer at T, and k_- with k^d indicating the rate constant of the melting of the de-oxygenated HbS polymer. So Eq.2 is rewritten as the following in term of the melting rate:

$$\frac{dC_m(t)}{dt} = -k^d \left(\frac{C_m(t)}{C_s} - 1 \right) C_p(t) \qquad (3)$$

Also, the total HbS molar concentration (C_{tot}) is the sum of the molar concentration of the hemoglobin

molecules in the polymer phase, C_p, and that in the monomer phase, C_m. $C_{\text{tot}}(t) = C_m(t) + C_p(t)$. After differentiating and substituting into Eq.3 with the fact that $\frac{dC_{\text{tot}}(t)}{dt} = 0$, we have:

$$\frac{dC_p(t)}{dt} = k^d \left(\frac{C_m(t)}{C_s} - 1 \right) C_p(t) \tag{4}$$

C. The Extended Model with Four Equations

With the CO-mediating the melting of the polymer incorporated [4], the polymerized and monomerized populations are then divided into two sub-populations: $C_p^{\text{CO}}(t)$ and $C_m^{\text{CO}}(t)$ which are CO-bound polymer and monomer HbS, respectively; and $C_p^d(t)$ and $C_m^d(t)$ which are de-oxy polymer and monomer HbS. Since CO binds to the monomer and polymer tightly, the model then assumes that CO-binding results in a decrease from de-oxy HbS $C_m^d(t)$ in the solution phase, which then becomes a gain for the CO-bound solution phase $C_m^{\text{CO}}(t)$, with a CO binding rate constant k_m. Taking all these into consideration produces Eq. 5. Likewise with the polymer phase molecules, the assumed CO-binding outcome is a loss from the $C_p^d(t)$ and a gain to $C_p^{\text{CO}}(t)$ by the CO binding rate constant k_p. Equation 6 corresponds to the production of CO-monomer. It is generated while making the same assumptions for the melting of the CO-polymer as the ones made when writing the differential equation of the melting of de-oxypolymer (Eq. 3), with the melting rate constant being K^{CO}, and the formation of the CO-monomer from deoxy monomer in the presence of CO with the rate constant being K_m. Equations 7 and 8 are produced the same way as Eq. 4 with taking into consideration the binding of CO to deoxy polymer. Our model is then based on the following:

$$\begin{aligned}\frac{dC_m^d(t)}{dt} &= -k^d \left(\frac{C_m^d(t)}{C_s} - 1 \right) C_p^d(t) \\ &\quad - k_m(\text{CO}) C_m^d(t) \end{aligned} \tag{5}$$

$$\begin{aligned}\frac{dC_m^{\text{CO}}(t)}{dt} &= k^{\text{CO}} \left(1 - \frac{C_m^{\text{CO}}(t)}{C_s^{\text{CO}}} \right) C_p^{\text{CO}}(t) \\ &\quad + k_m(\text{CO}) C_m^d(t) \end{aligned} \tag{6}$$

$$\begin{aligned}\frac{dC_p^d(t)}{dt} &= k^d \left(\frac{C_m^d(t)}{C_s} - 1 \right) C_p^d(t) \\ &\quad - k_p(\text{CO}) C_p^d(t) \end{aligned} \tag{7}$$

$$\begin{aligned}\frac{dC_p^{\text{CO}}(t)}{dt} &= -k^{\text{CO}} \left(1 - \frac{C_m^{\text{CO}}(t)}{C_s^{\text{CO}}} \right) C_p^{\text{CO}}(t) \\ &\quad + k_p(\text{CO}) C_p^d(t) \end{aligned} \tag{8}$$

These models allow CO-binding to polymers and melting occur at the endpoints as well as at the surfaces of polymer fibers [4]. The diagram in Fig. 2 describes the reaction paths in the model equations. With CO-binding, the de-oxygenated polymers/monomers of HbS produce CO polymers/monomers HbS. The melting/de-polymerization of the CO-bound or de-oxygenated polymers yields CO-bound de-oxygenated monomers, respectively in an equilibrium process.

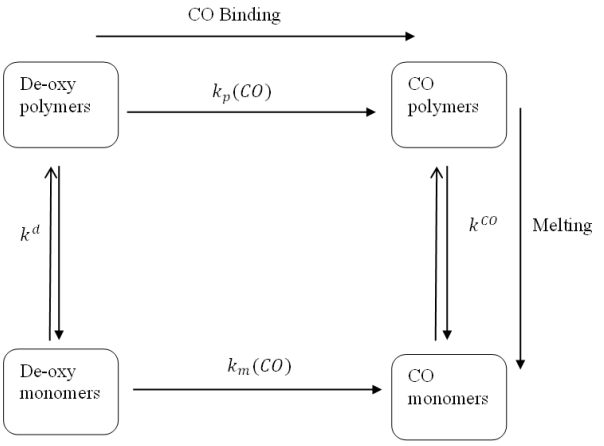

Fig. 2: The reaction paths of the CO-mediated de-polymerization of sickle cell HbS.

To mathematically analyze the system, we simplify the notations by replacing ($C_m^d(t)$, $C_m^{\text{CO}}(t)$, $C_p^d(t)$, $C_p^{\text{CO}}(t)$, k^d, $k_m(\text{CO})$, k^{CO}, $k_p(\text{CO})$, C_s, C_s^{CO}) by ($x(t)$, $y(t)$, $z(t)$, $u(t)$, k_1, k_2, k_3, k_4, C_1, C_2) respectively [10]. We then have the following model equations:

$$\frac{dx(t)}{dt} = -k_1 \left(\frac{x(t)}{C_1} - 1 \right) z(t) - k_2 x(t) \tag{9}$$

$$\frac{dy(t)}{dt} = k_3 \left(1 - \frac{y(t)}{C_2} \right) u(t) + k_2 x(t) \tag{10}$$

$$\frac{dz(t)}{dt} = k_1 \left(\frac{x(t)}{C_1} - 1 \right) z(t) - k_4 z(t) \tag{11}$$

$$\frac{du(t)}{dt} = -k_3 \left(1 - \frac{y(t)}{C_2} \right) u(t) + k_4 z(t) \tag{12}$$

III. Methodology

A. Traditional Sensitivity Analysis (TSA)

The traditional sensitivity functions (TSFs) are used in the traditional/classical sensitivity analysis. To investigate and quantify the sensitivity of a model output resulting from the variations in the parameters, we consider the partial derivatives of the output variable with respect to the parameters that it depends on [11,12]. The detailed TSFs for the sickle cell model in this study are derived and presented as follows.

Many times, the model is described by a system of ordinary differential equations (ODEs). The system can be written in the vector form:

$$\frac{dX(t)}{dt} = F(X, P) \tag{13}$$

where $X \in R^n$ denotes the state variable vector and $P \in R^r$ denotes the vector of parameters and the initial condition is $X(t_o) = X_o$. Depending on the research goal, the output variable vector Y for the sensitivity analysis can be a subset of X or the full state X. By sensitivity we mean how Y changes with respect to P, that is $\frac{\partial Y(t)}{\partial P}$. Since all the states are related and coupled, solving $\frac{\partial Y(t)}{\partial P}$ requires solving the full states $\frac{\partial X(t)}{\partial P}$. In the following, we work on the full state vector as the output variable vector. Note that as X is a function of time, the sensitivity is also a function of time. By differentiating both sides of Eq. 13 with respect to P, we have a system of differential equations for the sensitivities:

$$\frac{\partial}{\partial P}\frac{dX(t)}{dt} = \frac{\partial F}{\partial X}\frac{\partial X}{\partial P} + \frac{\partial F}{\partial P} \tag{14}$$

Now if we reverse the order of differentiation and couple the equation with Eq. 13 then we get a $n + nr$ dimensional system of ordinary differential equations for both the model variables and the sensitivities

$$\frac{dX(t)}{dt} = F(X, P) \tag{15}$$

$$\frac{d}{dt}\frac{\partial X}{\partial P} = \frac{\partial F}{\partial X}\frac{\partial X}{\partial P} + \frac{\partial F}{\partial P} \tag{16}$$

Here, we assume that $\frac{\partial X(0)}{\partial P} = 0$, because the initial conditions for the model would be considered independent of the parameters.

We apply the above Eqs. 15 and 16 onto our sickle cell model Eqs. 5–8. The new system is obtained with 4 original model equations and 16 equations for the TSFs. The detailed equations for the TSFs are presented in Appendix.

B. Multi-Parameter Sensitivity Analysis (MPSA)

First developed in the field of hydrology [13–15], the MPSA method is a technique that quantifies the relative importance of the parameters related to the output variables in the model [16]. The MPSA considers the combined effects of multiple parameters on the output of the model. We first use the Monte-Carlo method to randomly select values from the distributions of the considered parameters. Similar to the studies reported in [17, 18], we use the uniform probability distribution since the natural distribution of the parameters in the sickle cell polymer decomposition system is unknown. With the randomly selected parameters values, the differential equations model is then simulated repeatedly. Next, an objective value is calculated by using the objective function (defined below) to classify the output of the model simulation as either acceptable or unacceptable. Lastly, a statistical evaluation is carried out for the acceptable and unacceptable cases, giving quantified values for the sensitivities of the parameters.

The detailed procedure of the MPSA can be found in Cho et al. [16]. In this study, instead of setting the range between one fifth of a nominal value and five times the nominal value [16], for the sickle cell model, we set the range between one half of the nominal value and two times the nominal value since roughly speaking the rates may be doubled or halved when the temperature changes within ten degrees. In comparing the two cumulative distribution functions (CDF) of the parameter values associated with the acceptable and the unacceptable results, Cho et al. [16] simply consider the "cumulative frequencies" for each parameter via corresponding correlation coefficients. In this study, a more thorough comparison technique is adopted, namely, the Kolmogorov-Smirnov (KS) test [16]. The KS distance is calculated, with the large distance value indicating the large sensitivity of the parameter, since the large KS distance implies that the two CDFs are different to each other.

The objective value is defined as the sum of squared differences between the output values from the sampling parameters and the output values from the nominal parameters:

$$f_{\text{obj}}(k) = \sum_{i=1}^{q} \left(f_{\text{nominal}}(i) - f_{\text{sampling}}(i,k)\right)^2 \tag{17}$$

where $f_{\text{obj}}(k)$ is the objective function that describes how much the system output with the sampling parameters changes from the data with the nominal parameters; $f_{\text{nominal}}(i)$ denotes an output value from the nominal parameters at the ith time; $f_{\text{sampling}}(i,k)$ denotes the output value from the sampling parameter k at the ith time; and q is the number of time point.

IV. Results and Discussion

A typical solution behavior of the model over time and the general dynamics of the CO-mediated de-polymerization process can be seen in Fig. 3. The de-oxy monomer $x(t)$ first increases to its peak, then decreases gradually to 0, while the de-oxy polymer $z(t)$ decreases the whole time to 0. The CO-bound monomer $y(t)$ first increases to its peak which is higher than the

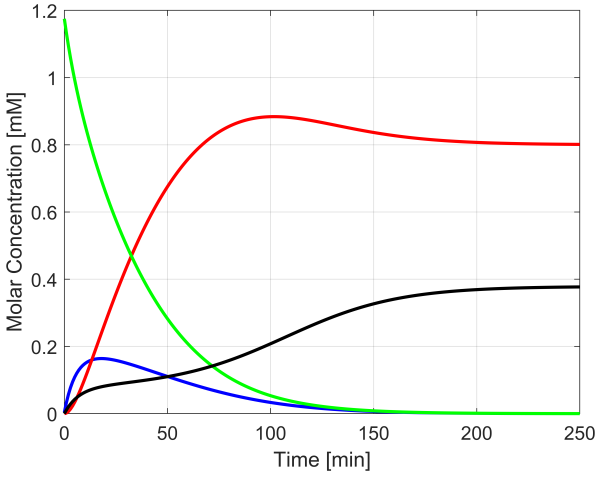

Fig. 3: Solution behavior of the model and dynamics of the CO-mediated de-polymerization process. Blue: de-oxy monomers x, red: CO-bound monomers y, green: de-oxy polymers z, black: CO-bound polymers u.

solubility, then decreases to its solubility, while the CO-bound polymer $u(t)$ increases the whole time to its solubility. For the solutions in Fig. 3, the parameters are set as $k_1 = 0.028$, $k_2 = 0.07$, $k_3 = 0.1$, $k_4 = 0.01$. The solubilities are $C_1 = 0.4$ and $C_2 = 0.8$. The initial conditions of the system are chosen as $x(0) = 0.0036$mM, $y(0) = 0$, $z(0) = 1.175$mM, $u(0) = 0$. A detailed analysis with rigorous mathematical proofs on the dynamics of the extended model Eqs. 9–12 can be found in Daniels-Jones et. al [10].

The above parameter values are set as the nominal values of the parameters. The above solubilities and initial conditions for Fig. 3 are used for the rest analysis in this study. The ranges of the parameters are set around the nominal values: $k_1 \in [0.014,\ 0.056]$, $k_2 \in [0.035,\ 0.014]$, $k_3 \in [0.05,\ 0.2]$, $k_4 \in [0.005,\ 0.02]$. The initial values and parameters ranges are chosen based on previous experimental studies on the CO-mediated sickle cell de-polymerization [2, 3]. Among all species, the initial concentration of de-oxy polymers $z(0)$ is the highest (1.175mM), because medically this is the species that causes sickle cell illness. The initial concentration of de-oxy monomer $x(0)$ being low value (0.0036mM) is justified due to the high value of de-oxy polymers. The initial concentrations of the other two species ($y(0)$ and $u(0)$) are assumed to be 0 because they are not exposed to the CO yet. Based on the model equations, the results remain similar for some range of initial and parameters values around the chosen ones. For very different initial and parameters values, the results of sensitivity may be different, which is not covered in this study. For the numerical simulations, we use the Runge-Kutta method for the time-marching integration of the ODEs, with time step $dt = 0.01$ and the time interval $[0,\ 400]$, which provides an adequate accuracy and sufficient transient time.

People often vary the parameter values and conduct experiments for responses to observe the effects of the parameters over the output variables. A rough estimate and some findings may be obtained in this way. As an example, with a few different k_1 values $(0.0112,\ 0.0224,\ 0.0336,\ 0.0448,\ 0.0560)$, the corresponding solutions of all four concentrations are presented in Fig. 4. From Fig. 4a, the increase of k_1 leads to the increase of the peak for x; the peak time remains the same; after the peak, the decreasing speed is large with a large k_1-value. From Fig. 4b, the larger the k_1-value is, the $y-$value increases faster to its higher peak (over the solubility 0.8), then decreases slower to 0.8 the solubility. From Fig. 4c, the larger the k_1-value is, the faster/quicker the z-value decreases to 0. Lastly, the u-value first increases slower with larger k_1-value. At some point of time, this is reversed: the u-value increases faster with larger k_1-value, as shown in Fig. 4d. It takes shorter time for the u-value to reach its solubility 0.4 with a larger k_1-value. The rough effect of the k_1-value on the individual variable can be observed in Fig. 4. However, some detailed sensitivity analysis, such as on which variable does the parameter k_1 have the most effect, cannot be obtained from Fig. 4 directly.

The effects of all four parameters over the variable CO-bound polymers concentration u are displayed in Fig. 5. All four parameters have some effects on variable u. From Fig. 5a and 5c for parameters k_1 and k_3, it starts with the lower the parameter values, the faster the u-value increases; after some time, this is reversed: the lower the parameter values, the slower the u-value increases. The solutions with various parameter values for k_2 and k_4 in Fig. 5b and 5d show the consistent trend: the lower the parameter values, the slower the u-value increases. The rough effect of the individual parameter over the u variable can be observed in Fig. 5. However, some detailed sensitivity analysis, such as which parameter has the most effect on the variable, cannot be obtained from Fig. 5 directly.

For a systematic sensitivity analysis and to compare the impacts of the parameters, we utilize the TSA and the MPSA to examine the sensitivities of the output variables (x, y, z, u) that are presented in our model equations with respect to the changes in the parameters' values (k_1, k_2, k_3, k_4). In the following 3 subsections,

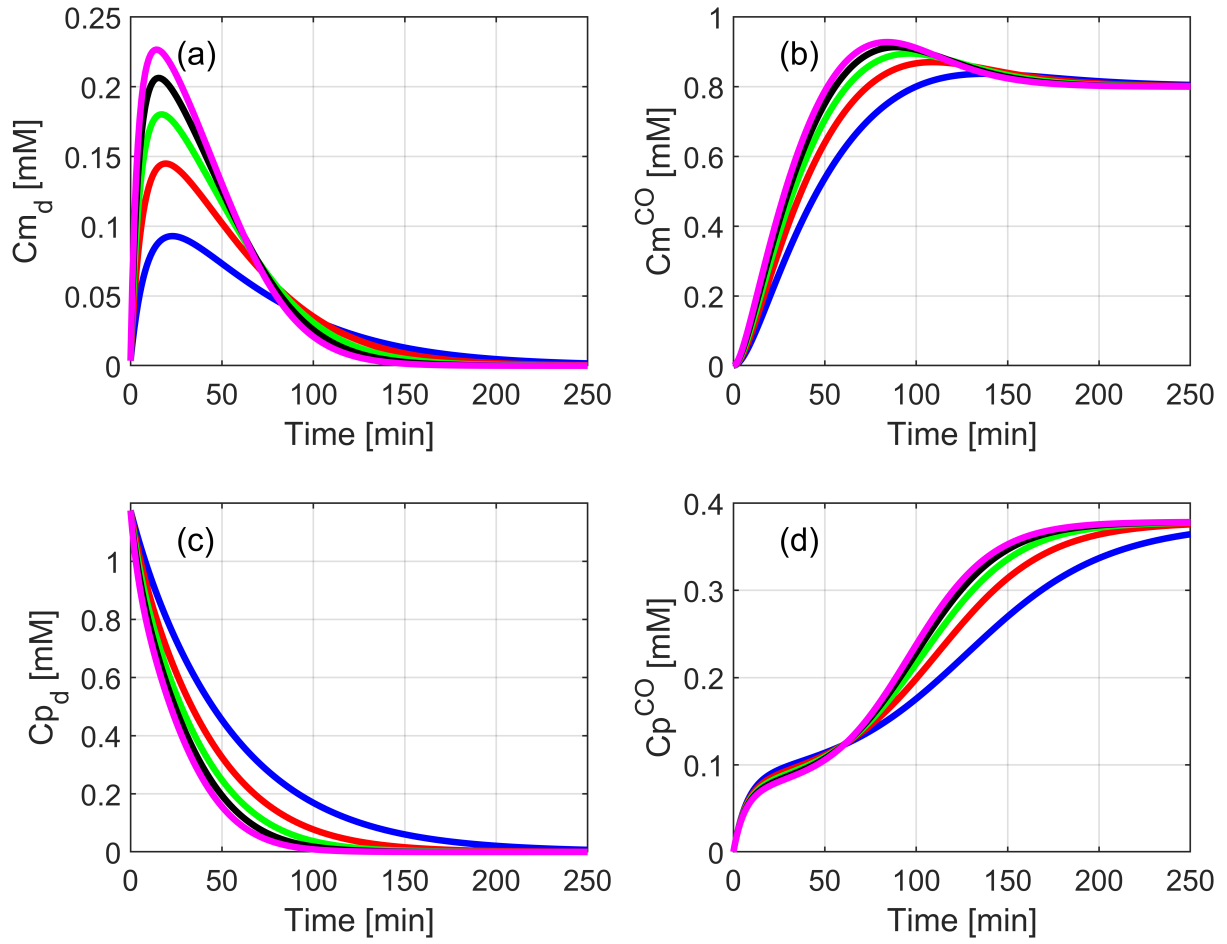

Fig. 4: The solutions of four concentrations when varying parameter k_1. blue: $k_1 = 0.0112$, red: $k_1 = 0.0224$, green: $k_1 = 0.0336$, black: $k_1 = 0.0448$, magenta: $k_1 = 0.056$. (a). de-oxy monomers x; (b). CO-bound monomers y; (c). de-oxy polymers z; (d). CO-bound polymers u.

we quantify the sensitivity with estimates, and we rank the effects of parameters accordingly.

A. Results from TSA

1) TSFs with parameters at nominal values: With the nominal values for the parameters, the ODEs for the TSF functions in Appendix can be solved numerically. Figure 6 shows the TSF functions $\left(\frac{\partial x}{\partial k_1}, \frac{\partial y}{\partial k_1}, \frac{\partial z}{\partial k_1}, \frac{\partial u}{\partial k_1}\right)$ of the variables with respect to parameter k_1. The behavior of the TSFs in Fig. 6 is consistent with the phenomenon in Fig. 4. The larger the TSF value is, the larger the sensitivity (change/variation) of the variable is. The positive TSF value means that the increase of the parameter leads to the increase of the variable value, while the negative TSF value means the opposite. From Fig. 6a for the sensitivity of variable x over parameter k_1, the sensitivity increases to its peak at $t \approx 20$, then decreases to 0 at $t \approx 75$, continues to decrease and then increases but remains negative, lastly at $t \approx 200$ it settles at 0. The time stamps $(20, 75, 200)$ match well with those in Fig. 4a. Similar consistency can be found in Fig. 6b vs Fig. 4b, in Fig. 6c vs Fig. 4c, and in Fig. 6d vs Fig. 4d. It should be noted that all the sensitivities converge asymptotically to 0 over some time. Note that instead of the discrete values for the parameter in the trials in Fig. 4, the TSF describes the instantaneous change/impact of the variable with respect to the change (increase or decrease) in the parameter. Therefore, as a quantified sensitivity, the TSF in Fig. 6 is more rigorous and more reliable than the rough estimate observed from Fig. 4.

The sensitivities presented in Fig. 6 are functions of time, i.e., the sensitivity values are different at different times. To better compute the sensitivity of the variable

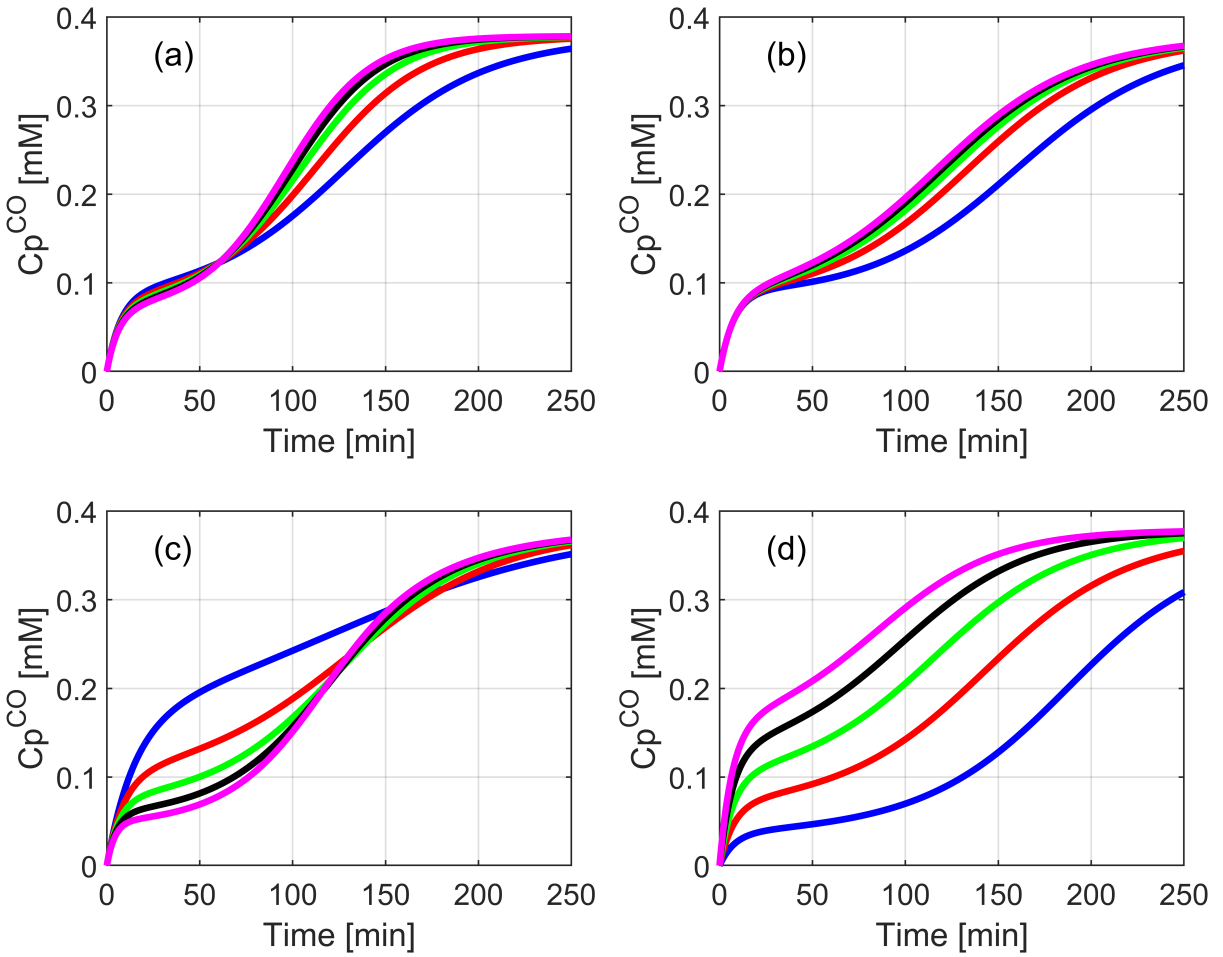

Fig. 5: The response of CO-bound polymers concentration u when varying parameters. (a). Various k_1, blue: $k_1 = 0.0112$, red: $k_1 = 0.0224$, green: $k_1 = 0.0336$, black: $k_1 = 0.0448$, magenta: $k_1 = 0.056$. (b). Various k_2, blue: $k_2 = 0.028$, red: $k_2 = 0.056$, green: $k_2 = 0.084$, black: $k_2 = 0.112$, magenta: $k_2 = 0.14$. (c). Various k_3, blue: $k_3 = 0.04$, red: $k_3 = 0.08$, green: $k_3 = 0.12$, black: $k_3 = 0.16$, magenta: $k_3 = 0.2$. (d). Various k_4, blue: $k_4 = 0.004$, red: $k_4 = 0.008$, green: $k_4 = 0.012$, black: $k_4 = 0.016$, magenta: $k_4 = 0.02$.

to the parameter, we sum up the sensitivity values over the time. For this analysis, we use the L^2 norm of the TSF to measure the sensitivity. Note this norm is defined as [11]:

$$\|f\|_2^2 = \int_a^b f^2(t)dt \tag{18}$$

Since we are approximating the solution to our sensitivity $\frac{\partial X}{\partial P}$, we also approximate this norm. The L^2 norms of the TSFs are shown in Table I.

With the quantified sensitivity values in Table I, we can compare and rank the sensitivities of variables to the parameter by reading the table in columns. The column of k_1 for the sensitivities of variables to the parameter k_1 shows that variable z is the most sensitive, followed by y. The sensitivities of u and x variables are similar. The sensitivity values in column k_1 quantify the phenomenon in Fig. 4, sum up the values in Fig. 6, and are consistent with the figures. Note that the scales in the vertical axes in Figs. 4 and 6 vary. All the sensitivity values in column k_2 are smaller than those in column k_1, which implies that k_2 may not affect the variables as much as k_1. The effect of k_3 is simple with 0 sensitivity for variables x and z, and some small sensitivity for the other two variables. The values in k_4 column are large, indicating the large effect on all variables. In a summary, from the columns in Table I, the order of variables' sensitivities (from large to small) is (z, y, u, x) for k_1; (x, y, u, z) for k_2; ($u - y$, $x - z$) for k_3; and (u, z, y, x) for k_4, where the dash "$-$" means the same sensitivity.

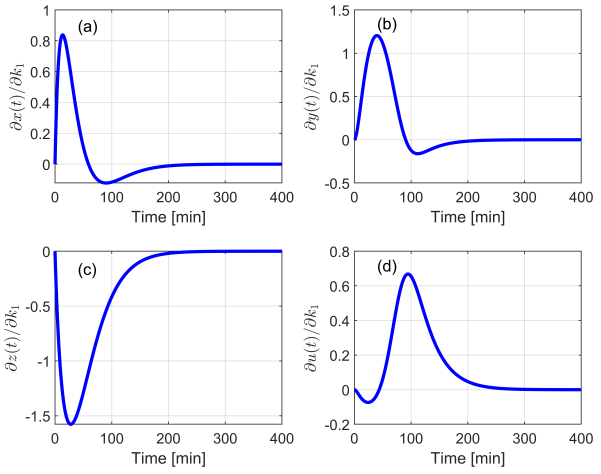

Fig. 6: The TSF functions of variables with respect to parameter k_1 with the nominal values for the parameters. (a) the TSF of variable $x(t)$ with respect to k_1, $\frac{\partial x(t)}{\partial k_1}$; b) the TSF of variable $y(t)$ with respect to k_1, $\frac{\partial y(t)}{\partial k_1}$; c) the TSF of variable $z(t)$ with respect to k_1, $\frac{\partial z(t)}{\partial k_1}$; d) the TSF of variable $u(t)$ with respect to k_1, $\frac{\partial u(t)}{\partial k_1}$.

Reading in rows of Table I, we can compare and rank the sensitivities of the variable to parameters. In row x, parameter k_4 is with the largest sensitivity, followed by k_1 and then k_2. k_3 has no effect on variable x. From the other rows for the other variables, even though the sensitivity values are different, but the order of parameters is consistent: k_4, k_1, k_2, k_3. Note that the values in row u in Table I quantify the variation in Fig. 5 for variable u with different varying parameters. The measure provided in Table I is more reliable and clearer than the rough variation in Fig. 5. The order/rank of the parameters (k_4, k_1, k_2, k_3) may not be obtained directly from Fig. 5.

2) TSFs when all parameter values vary: The above sensitivities are measured for the nominal values of the parameters. With different parameters' values, the changes on the variables are different. Figure 7 shows the variations of the variables for various parameter values in the ranges around the nominal values. The reference variable values are the solutions when the parameters are at the nominal values. For Fig. 7, the parameters' values are chosen randomly from the ranges of the parameters. Therefore, the effects of the combinations of the parameters are presented in Fig. 7.

It can be seen from Fig. 7 that the solution values vary above and below the reference values with different values for the parameters. However, it is not easy to analyze the sensitivity behavior directly from

Variables	k_1	k_2	k_3	k_4
x	41.5601	25.9384	0	44.3415
y	77.1920	20.7210	10.3865	100.7236
z	113.7541	1.9437	0	128.8967
u	47.7038	20.0600	10.3865	203.1208

Table I: TSA results: the sensitivities when parameters are nominal values.

Variables	k_1	k_2	k_3	k_4
x	0.6195	0.9640	0	0.0772
y	1.0130	0.8312	0.4162	0.7778
z	1.5828	0.0025	0	0.7172
u	1.0570	0.9943	0.4162	1.9409

Table II: TSA results: the sensitivities when all parameters vary.

Fig. 7. To quantify the measure of the sensitivities, we utilize the TSFs. As an example, Fig. 8 shows the TSFs of all variables with respect to parameter k_1 when all parameters are varied. The behavior of the graphs follows a similar pattern due to the increase or the decrease of the parameters' values.

Next, to wrap up the results in Fig. 8, we semi-normalize the TSFs. Normalization is a process that is used to eliminate redundancy, reduce the potential for anomalies during data processing and maintain the consistency and integrity of the data. The L^2 norm of the TSF with the sampling parameters referenced to the TSF with the nominal parameters is given

$$\left\| \frac{\partial X}{\partial P}|_{P=P_s} - \frac{\partial X}{\partial P}|_{P=P_o} \right\|_2^2 = \sum_i \left(\left| \frac{\partial X(t_i)}{\partial P}|_{P=P_s} - \frac{\partial X(t_i)}{\partial P}|_{P=P_o} \right|^2 \cdot \Delta t \right) \tag{19}$$

where $X = \{x, y, z, u\}'$, $P = \{k_1, k_2, k_3, k_4\}'$, P_s is the sampled parameter value, and P_o is the nominal value. The semi-normalizer consists of multiplying the norm by the distance between the parameters. It is defined as follows:

$$\sum_j \left(|P_{s_j} - P_o| \left\| \frac{\partial X}{\partial P}|_{P=P_{S_j}} - \frac{\partial X}{\partial P}|_{P=P_o} \right\|_2 \right) \tag{20}$$

The results, the semi-normalization norm for the TSFs of each variable and each parameter is reported in Table II. The values in Table II measure the difference between the magnitudes of TSFs. The larger the value is, the larger difference between the magnitudes of the TSFs is, thus the more sensitive the variable is to the parameter.

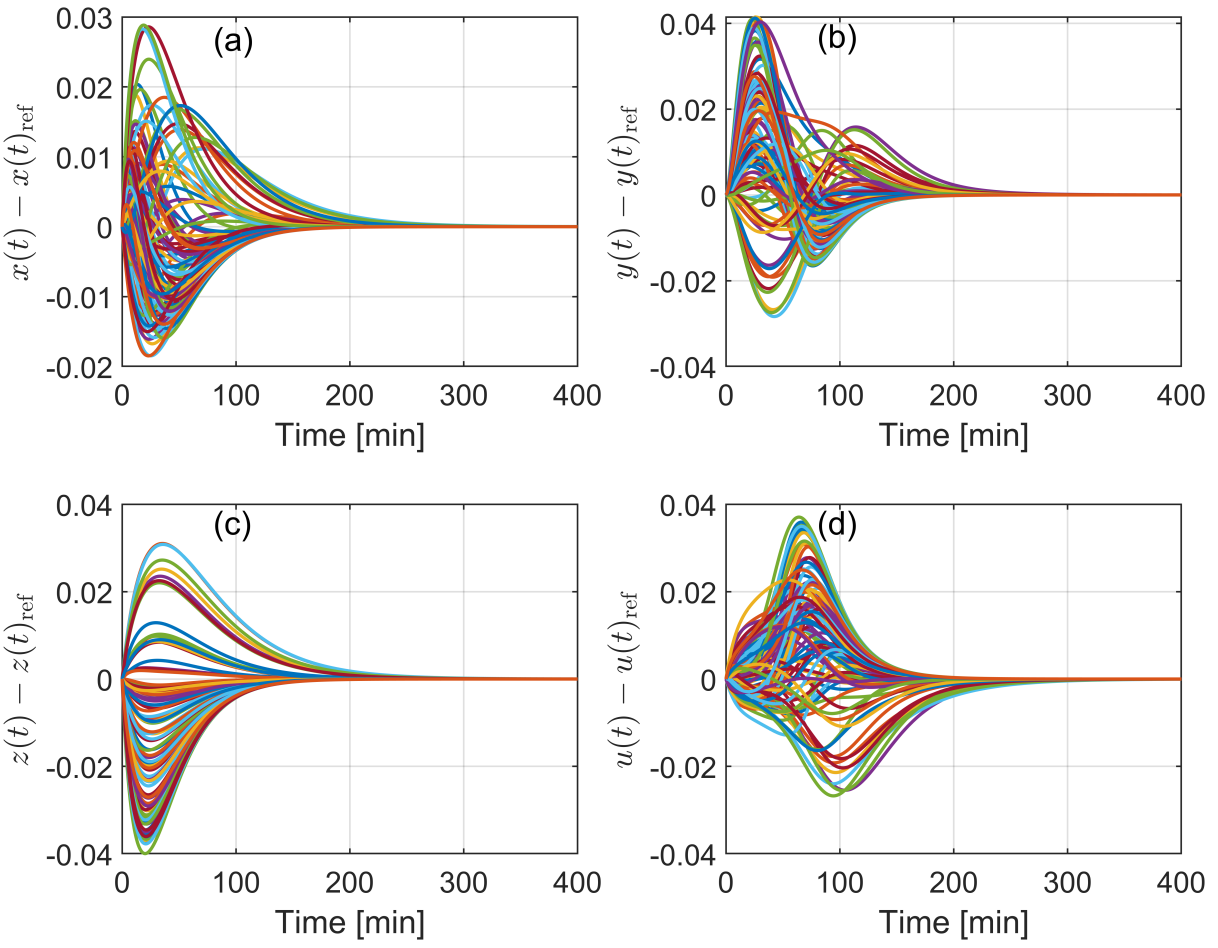

Fig. 7: The variations of the variables with various parameters' values in the ranges around the nominal values. The reference values are the solutions when the nominal values are set in the model equations. (a). The $x(t)-$ variation with various parameters' values; (b). The $y(t)-$ variation with various parameters' values; (c). The $z(t)-$ variation with various parameters' values; (d). The $u(t)-$ variation with various parameters' values.

Compared with Table I, the rankings of the sensitivities in Table II for variables and for parameters are different. Reading in columns, the ranking of the variables (from high to low) is z, u, y, x for k_1; u, x, y, z for k_2; (y, u), (x, z) for k_3; u, y, z, x for k_4. Reading in rows, the ranking of the parameters (from high to low) is k_2, k_1, k_4, k_3 for x; k_1, k_2, k_4, k_3 for y; k_1, k_4, k_2, k_3 for z; k_4, k_1, k_2, k_3 for u.

B. Results from MPSA

We use the random values following the uniform distribution for the sampling of parameters k_1, k_2, k_3, k_4. The sample size is 10,000 points. In other words, we take random values within the ranges of k_1, k_2, k_3, k_4 10,000 times and simulate the differential equations (DEs) system 10,000 times. Six (6) different percentiles including, the 25^{th}, 37.5^{th}, 50^{th}, 62.5^{th}, 75^{th} and the mean of the objective function values are chosen as the criteria to classify the cases as acceptable or unacceptable in the computation of the probability mass functions (PMFs) and the cumulative distribution functions (CDFs). Nonetheless, the rank of the sensitivity of x with respect to each parameter remains the same for each chosen percentile and the mean. The results from larger size samplings are essentially identical to the results reported here.

In this study, we plot out all the PMFs and CDFs of acceptance and non-acceptance of four parameters for four variables. Here, we choose the variable y for a detailed analysis. Similar discussions are carried out for the other variables, and the figures are omitted here. The PMFs of acceptance and non-acceptance of parameter

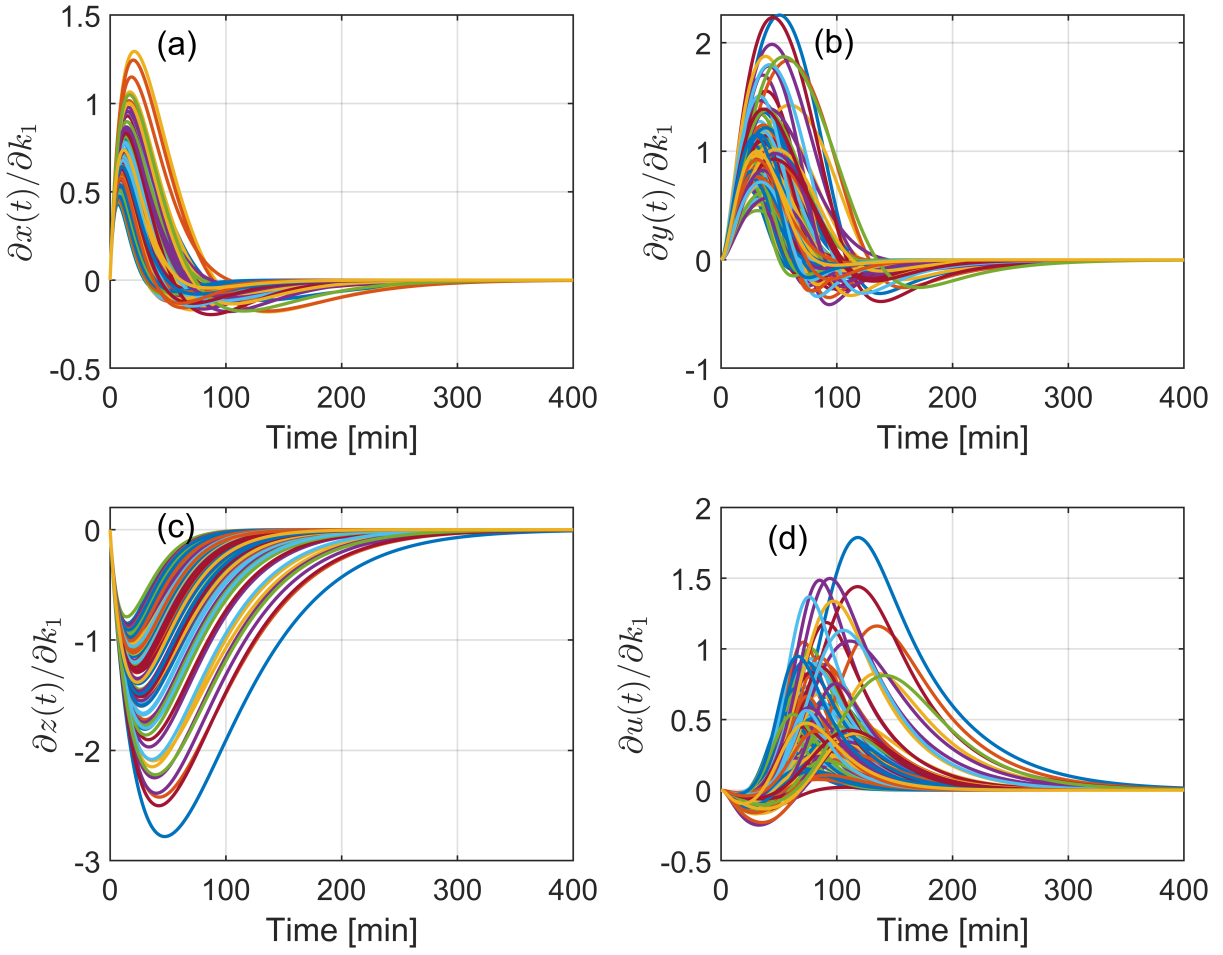

Fig. 8: The TSFs for all variables with respect to parameter k_1 when all parameters vary. (a) the TSF of variable $x(t)$ with respect to k_1, $\frac{\partial x(t)}{\partial k_1}$; b) the TSF of variable $y(t)$ with respect to k_1, $\frac{\partial y(t)}{\partial k_1}$; c) the TSF of variable $z(t)$ with respect to k_1, $\frac{\partial z(t)}{\partial k_1}$; d) the TSF of variable $u(t)$ with respect to k_1, $\frac{\partial u(t)}{\partial k_1}$.

k_1 for variable y are presented in the Fig. 9, and their CDFs of acceptance and non-acceptance are displayed in Fig. 10. The PMFs and CDFs of other parameters are similar to Figs. 9 and 10. The distributions are tested, and the Kolmogorov-Smirnov distance is computed to rank the sensitivity of each parameter, with the results shown in Table III. From these results including the figures and the table, for the output variable y the ranking of all four parameters sensitivities is k_1, k_2, k_3, k_4. From the values in Table III and the graphs in Figs. 11 and 12 for the PMFs and CDFs of all four parameters for variable y, the sensitivity of parameters k_3 and k_4 are very close with no significant difference.

Similarly to the analysis on the output variable y in the above, we compute the PMFs of acceptance and non-acceptance, the CDFs of acceptance and non-acceptance, and the Kolmogorov-Smirnov distances for each output variables x, z, and u. Since the rank of the sensitivity of each parameter remains the same in each chosen percentile (the 25^{th}, the 37.5^{th}, the 50^{th}, the 62.5^{th}, the 75^{th}) and the mean of the objectives for one variable, we choose the mean values of the objectives for each variable to report in detail in Table IV. From Table IV, with the output variable y the ranking for all four parameters sensitivities is k_1, k_2, k_3, k_4; with variable z the sensitivity ranking is k_1, k_4, k_2, k_3; with variable u the sensitivity ranking is k_4, k_2, k_1, k_3.

C. Comparison of the results from TSA and MPSA

In comparison of the results from the TSA and MPSA methods, Table V displays the ordering of the ranks. Here, we notice that both results are consistent

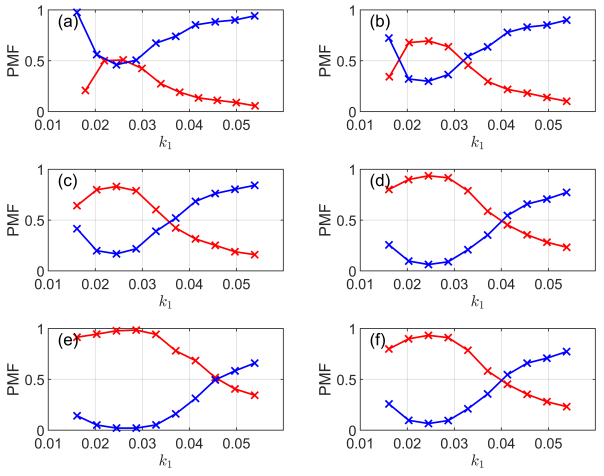

Fig. 9: The PMFs of acceptable (red) and unacceptable (blue) cases of parameter k_1 for variable y, in different level of percentile objectives. (a). The 25^{th} percentile; (b). The 37.5^{th} percentile; (c). The 50^{th} percentile; (d). The 62.5^{th} percentile; (e). The 75^{th} percentile; (f). Mean.

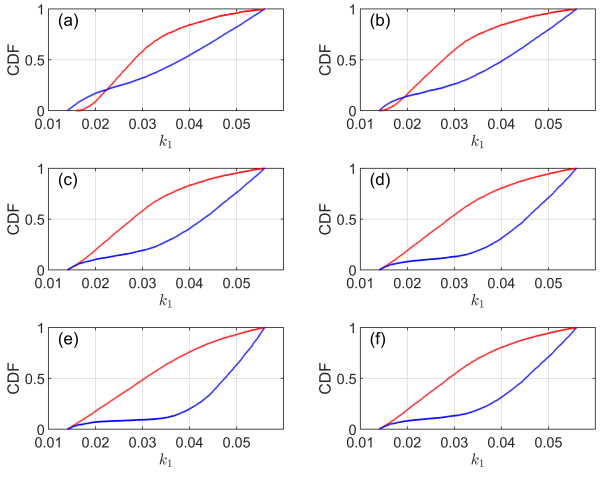

Fig. 10: The CDFs of acceptable (red) and unacceptable (blue) cases of parameter k_1 for variable y, in different level of percentile objectives. (a). The 25^{th} percentile; (b). The 37.5^{th} percentile; (c). The 50^{th} percentile; (d). The 62.5^{th} percentile; (e). The 75^{th} percentile; (f). Mean.

except for the output variable y whose 3^{nd} and 4^{rd} sensitivity ranks are reversed in the TSA and MPSA methods, and the variable u whose 2^{nd} and 3^{rd} sensitivity ranks are also reversed in the TSA and MPSA methods. Nevertheless, the variable x is most sensitive to changes in the parameter k_2, the variable y and z are most sensitive to changes in the parameter k_1, and the variable u is most sensitive to changes in the parameter k_4. k_3 does not affect any output variable significantly.

Percentile	k_1	k_2	k_3	k_4
25^{th} percentile	0.3060	0.2864	0.1005	0.1111
37.5^{th} percentile	0.3723	0.2804	0.0831	0.0604
50^{th} percentile	0.4514	0.2844	0.0770	0.0608
62.5^{th} percentile	0.5103	0.3160	0.0721	0.0660
75^{th} percentile	0.5757	0.3877	0.0767	0.0744
Mean of objectives	0.5097	0.3150	0.0730	0.0653

Table III: MPSA results: ranks of all parameters for variable x at various percentile objectives.

Variables	k_1	k_2	k_3	k_4
x	0.0942	0.3389	0.0235	0.0870
y	0.5097	0.3150	0.0730	0.0653
z	0.6505	0.0211	0.0205	0.0958
u	0.1996	0.2837	0.1135	0.3681

Table IV: MPSA results: mean of the objectives for all parameters with variables.

V. Conclusion and Future Topics

From the previous studies [3,4], the melting of HbS polymers into monomers is beneficial, if not mandatory to eliminate the sickling of the red blood cell. Furthermore, carbon monoxide (CO) has been shown to improve the process of HbS polymers melting. Sangart Inc. (San Diego, CA) [19] has developed a drug called MP4CO that delivers CO at a therapeutic level to the sickle cells to facilitate the melting process. In the extended model [4], we see that many parameters play important roles in the breaking down of the de-oxy HbS polymers which leads to the formation of the CO-bound HbS monomers. Thus, it is crucial to determine the most important parameters that affect de-oxy HbS polymers and the CO-bound HbS monomers. Therefore, we analyze the sensitivity of all parameters to identify the most important parameters in the de-polymerization process.

Our first set of numerical experiments addresses the sensitivity of the variables with respect to the parameters using the TSA method. The representatives of sensitivity graphs are plotted as functions of time in Fig. 6 for CO monomers. The sensitivity values using the L^2 norms of the TSFs are displayed in Table I, which shows the strong effect of the CO-binding rate to de-oxygenated polymers (k_p(CO) on all the variables, i.e., the most sensitive parameter. The melting rate of CO-bound polymers (k^{CO}) shows a weak effect on the variables, thus it appears to be the least sensitive or insensitive. Therefore, the concentration of de-oxygenated HbS polymers and the concentration of

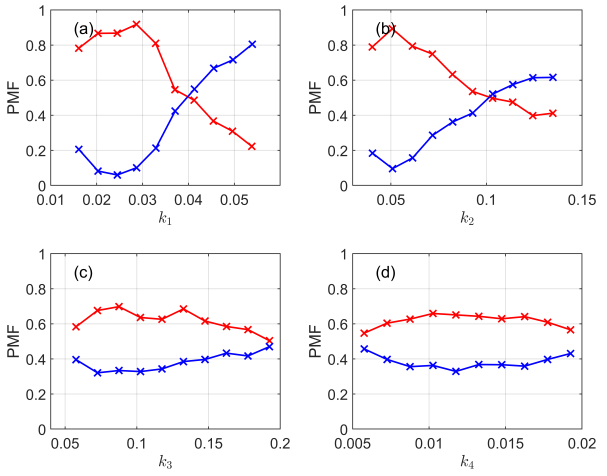

Fig. 11: The PMFs of acceptable (red) and unacceptable (blue) cases of all parameters for variable y, in the mean of percentile objectives. (a). Parameter k_1; (b). Parameter k_2; (c). Parameter k_3; (d). Parameter k_4.

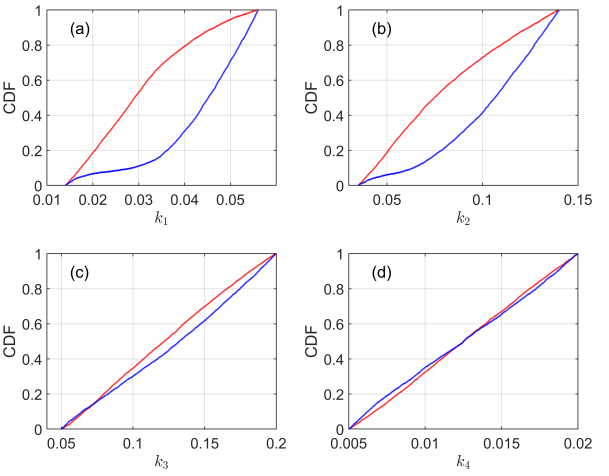

Fig. 12: The CDFs of acceptable (red) and unacceptable (blue) cases of all parameters for variable y, in the mean of percentile objectives. (a). Parameter k_1; (b). Parameter k_2; (c). Parameter k_3; (d). Parameter k_4.

CO-bound HbS monomers are affected the most by the rate $k_p(\mathrm{CO})$ and the least by k^{CO}.

In the next analysis, using the previous TSFs, we study the sensitivities while all parameters are varied. As all the parameters are varied simultaneously, we notice quite a change in the sensitivity rankings. Here, we notice the importance of melting rate of de-oxygenated polymers (k^d) on the concentration of de-oxygenated HbS polymers and CO-bound HbS monomers. It should be noted that the k^d is the most important parameter in the breaking down of the de-oxygenated HbS polymers and the formation of the CO-bound HbS monomers. Followed by k^d, $k_p(\mathrm{CO})$ is the second sensitive parameter to the concentration of de-oxygenated HbS polymers and $k_m(\mathrm{CO})$ is the second sensitive parameter to the concentration of CO-bound HbS monomers. As for the concentration of de-oxy HbS monomers, $k_m(\mathrm{CO})$ followed by k^d are the two most sensitive parameters. For the concentration of CO-bound HbS polymers $k_p(\mathrm{CO})$ is the parameter that causes the most disturbance. It should be noted that k^{CO} has demonstrated the weakest effect in the sensitivity of all output variables.

Lastly, we perform the MPSA on the CO-mediated sickle cell de-polymerization with the same set of initial conditions and parameter ranges. The sensitivity rankings of all output values with respect to all input parameters are obtained by the MPSA analysis directly. These results are essentially identical to the results from TSA with semi-normalization of the TSFs.

In comparing the methods of sensitivity analysis employed in this study, both TSA and MPSA have pros and cons. The TSA method is simple to derive mathematically and simple to implement in the program codes to obtain the TSFs numerically. But it is limited by its large computational cost. In a case where there are many parameters (r) and output variables (n), there will be many equations ($n + n \times r$) for the TSFs. The TSA also focuses on the local effect of the parameter on the output variables. As for the MPSA method, multiple parameters can be considered at the same time. This method studies the overall effect of the parameters on the output's variables. The disadvantage of this method is the large size of sampling for the parameters because of the Monte-Carlo simulation.

In chemical reactions, temperature plays an important role. The fluctuation of temperature influences the rate of reactions. The rate constants present in the model are influenced by the temperature variation [20]. Sensitivity analyses, such as the TSA and MPSA performed in this study, are useful tools in the iterative mathematical modeling process. Results from the sensitivity analysis can be used to inform and design future experiments, whose results can be used to further refine the mathematical model. In this study for CO-mediated sickle cell de-polymerization, the results indicate that the system shows the most sensitivity within the first 200 minutes. The system seems to approach the same equilibria regardless of the parameters chosen, which suggests that additional experimentation should focus on obtaining data during the first 200 minutes. Furthermore, this study suggests that the system is most sensitive to the melting rate of the de-oxygenated polymer (k_d),

Variables	Sensitivity Analysis Method	Ranking Order
x	TSA	$k_2 - k_1 - k_4 - k_3$
x	MPSA	$k_2 - k_1 - k_4 - k_3$
y	TSA	$k_1 - k_2 - k_4 - k_3$
y	MPSA	$k_1 - k_2 - k_3 - k_4$
z	TSA	$k_1 - k_4 - k_2 - k_3$
z	MPSA	$k_1 - k_4 - k_2 - k_3$
u	TSA	$k_4 - k_1 - k_2 - k_3$
u	MPSA	$k_4 - k_2 - k_1 - k_3$

Table V: Ranking results of TSA and MPSA.

followed by the CO binding rates for monomers and polymers (k_m(CO), k_p(CO)). The system shows little sensitivity to the melting rate of the CO polymer (k^{CO}). Future experimentation that investigates these rates would be useful to further verify these results.

For the future topics, first of all, both the TSA and MPSA analyses can be conducted for the initial conditions $C_m^d(0)$, $C_m^{\text{CO}}(0)$, $C_p^d(0)$, and $C_p^{\text{CO}}(0)$, and the solubilities C_s, C_s^{CO}, for each output variable $C_m^d(t)$, $C_m^{\text{CO}}(t)$, $C_p^d(t)$, and $C_p^{\text{CO}}(t)$. Secondly, it can be seen from the analysis in this study that the sensitivity values calculated by the L^2 norm of the TSFs are affected by the scales of the functions. Instead of the TSFs, we may use the relative sensitivity functions for a more delicate study. More details of the relative sensitivity functions can be found in [5,6]. Thirdly and lastly, the MPSA can be further improved. For example, the K-S measuring is a rough approximation for the distance between two CDFs. A more delicate technique may be developed to measure the difference between the acceptance and non-acceptance distributions. Another example, if there exists appreciable correlation between parameters, the current version MPSA may not be efficient. Taking the correlation of parameters into consideration, we may project the distributions onto new axes to obtain a more accurate result.

VI. Software availability

The analysis in this study has been done in Matlab. The whole set of Matlab codes are uploaded and published on GitHub at the following link: https://github.com/lipingliuncat/ParameterSensitivity.

VII. Acknowledgement

This study is supported by the Department of Mathematics and Statistics at North Carolina Agricultural and Technical State University. The authors greatly appreciate the detailed comments and suggestions made by the editor and reviewers, which significantly improved the work.

VIII. Appendix

The sensitivity equations for all four parameters:

$$\frac{dx(t)}{dt} = -k_1\left(\frac{x(t)}{C_1} - 1\right)z(t) - k_2 x(t)$$

$$\frac{d}{dt}\frac{\partial x}{\partial k_1} = \left(1 - \frac{x(t)}{C_1}\right)z(t) + k_1\left(1 - \frac{x(t)}{C_1}\right)\frac{\partial z(t)}{\partial k_1} - k_1\frac{1}{C_1}\frac{\partial x(t)}{\partial k_1}z(t) - k_2\frac{\partial x(t)}{\partial k_1}$$

$$\frac{d}{dt}\frac{\partial x}{\partial k_2} = k_1\left(1 - \frac{x(t)}{C_1}\right)\frac{\partial z(t)}{\partial k_2} - k_1\frac{1}{C_1}\frac{\partial x(t)}{\partial k_2}z(t) - k_2\frac{\partial x(t)}{\partial k_2} - x(t)$$

$$\frac{d}{dt}\frac{\partial x}{\partial k_3} = k_1\left(1 - \frac{x(t)}{C_1}\right)\frac{\partial z(t)}{\partial k_3} - k_1\frac{1}{C_1}\frac{\partial x(t)}{\partial k_3}z(t) - k_2\frac{\partial x(t)}{\partial k_3}$$

$$\frac{d}{dt}\frac{\partial x}{\partial k_4} = k_1\left(1 - \frac{x(t)}{C_1}\right)\frac{\partial z(t)}{\partial k_4} - k_1\frac{1}{C_1}\frac{\partial x(t)}{\partial k_4}z(t) - k_2\frac{\partial x(t)}{\partial k_4}$$

$$\frac{dy(t)}{dt} = k_3\left(1 - \frac{y(t)}{C_2}\right)u(t) + k_2 x(t)$$

$$\frac{d}{dt}\frac{\partial y}{\partial k_1} = k_3\left(1 - \frac{y(t)}{C_2}\right)\frac{\partial u(t)}{\partial k_1} - k_3\frac{1}{C_2}\frac{\partial y(t)}{\partial k_1}u(t) + k_2\frac{\partial x(t)}{\partial k_1}$$

$$\frac{d}{dt}\frac{\partial y}{\partial k_2} = k_3\left(1 - \frac{y(t)}{C_2}\right)\frac{\partial u(t)}{\partial k_2} - k_3\frac{1}{C_2}\frac{\partial y(t)}{\partial k_2}u(t) + k_2\frac{\partial x(t)}{\partial k_2} + x(t)$$

$$\frac{d}{dt}\frac{\partial y}{\partial k_3} = \left(1 - \frac{y(t)}{C_2}\right)u(t) + k_3\left(1 - \frac{y(t)}{C_2}\right)\frac{\partial u(t)}{\partial k_3} - k_3\frac{1}{C_2}\frac{\partial y(t)}{\partial k_3}u(t) + k_2\frac{\partial x(t)}{\partial k_3}$$

$$\frac{d}{dt}\frac{\partial y}{\partial k_4} = k_3\left(1 - \frac{y(t)}{C_2}\right)\frac{\partial u(t)}{\partial k_4} - k_3\frac{1}{C_2}\frac{\partial y(t)}{\partial k_4}u(t) + k_2\frac{\partial x(t)}{\partial k_4}$$

$$\frac{dz(t)}{dt} = k_1\left(\frac{x(t)}{C_1} - 1\right)z(t) - k_4 z(t)$$

$$\frac{d}{dt}\frac{\partial z}{\partial k_1} = \left(\frac{x(t)}{C_1} - 1\right)z(t) + k_1\left(\frac{x(t)}{C_1} - 1\right)\frac{\partial z(t)}{\partial k_1} + k_1\frac{1}{C_1}\frac{\partial x(t)}{\partial k_1}z(t) - k_4\frac{\partial z(t)}{\partial k_1}$$

$$\frac{d}{dt}\frac{\partial z}{\partial k_2} = k_1\left(\frac{x(t)}{C_1}-1\right)\frac{\partial z(t)}{\partial k_2} + k_1\frac{1}{C_1}\frac{\partial x(t)}{\partial k_2}z(t) - k_4\frac{\partial z(t)}{\partial k_2}$$

$$\frac{d}{dt}\frac{\partial z}{\partial k_3} = k_1\left(\frac{x(t)}{C_1}-1\right)\frac{\partial z(t)}{\partial k_3} + k_1\frac{1}{C_1}\frac{\partial x(t)}{\partial k_3}z(t) - k_4\frac{\partial z(t)}{\partial k_3}$$

$$\frac{d}{dt}\frac{\partial z}{\partial k_4} = k_1\left(\frac{x(t)}{C_1}-1\right)\frac{\partial z(t)}{\partial k_4} + k_1\frac{1}{C_1}\frac{\partial x(t)}{\partial k_4}z(t) - k_4\frac{\partial z(t)}{\partial k_4} - z(t)$$

$$\frac{du(t)}{dt} = -k_3\left(1-\frac{y(t)}{C_2}\right)u(t) + k_4 z(t)$$

$$\frac{d}{dt}\frac{\partial u}{\partial k_1} = -k_3\left(1-\frac{y(t)}{C_2}\right)\frac{\partial u(t)}{\partial k_1} + k_3\frac{1}{C_2}\frac{\partial y(t)}{\partial k_1}u(t) + k_4\frac{\partial z(t)}{\partial k_1}$$

$$\frac{d}{dt}\frac{\partial u}{\partial k_2} = -k_3\left(1-\frac{y(t)}{C_2}\right)\frac{\partial u(t)}{\partial k_2} + k_3\frac{1}{C_2}\frac{\partial y(t)}{\partial k_2}u(t) + k_4\frac{\partial z(t)}{\partial k_2}$$

$$\frac{d}{dt}\frac{\partial u}{\partial k_3} = -\left(1-\frac{y(t)}{C_2}\right)u(t) - k_3\left(1-\frac{y(t)}{C_2}\right)\frac{\partial u(t)}{\partial k_3} + k_3\frac{1}{C_2}\frac{\partial y(t)}{\partial k_3}u(t) + k_4\frac{\partial z(t)}{\partial k_3}$$

$$\frac{d}{dt}\frac{\partial u}{\partial k_4} = -k_3\left(1-\frac{y(t)}{C_2}\right)\frac{\partial u(t)}{\partial k_4} + k_3\frac{1}{C_2}\frac{\partial y(t)}{\partial k_4}u(t) + k_4\frac{\partial z(t)}{\partial k_4} + z(t)$$

REFERENCES

[1] V. M. Ingram, A specific chemical difference between the globins of normal human and sickle cell anemia hemoglobin, *Nature*, 178:792–794, 1956.

[2] S. K. Aroutiounian, J. G. Louderback, S. K. Ballas, D. B. Kim-Shapiro, Evidence for carbon monoxide binding to sickle cell polymers during melting, *Biophysical Chemistry*, 91:167–181, 2001.

[3] F. A. Ferrone, J. Hofrichter, W. A. Eaton, Kinetics of sickle hemoglobin polymerization II: A double nucleation mechanism, *Journal of Molecular Biology*, 183:611–631, 1985.

[4] M. Chen, D. P. Clemence, G. Gibson, Analysis of numerical schemes of a mathematical model for sickle cell depolymerization, *Applied Mathematics and Computation*, 216:1489–1500, 2010.

[5] Z. Zi, Sensitivity analysis approaches applied to systems biology models, *IET Systems Biology*, 5:336–346, 2011.

[6] A. Saltelli, M. Ratto, T. Andres, F. Campolongo, J. Cariboni, D. Gatelli, M. Saisana, S. Tarantola, *Global Sensitivity Analysis: The Primer*, John Wiley & Sons, 2008.

[7] A. Raue, C. Kreutz, T. Maiwald, U. Klingmuller, J. Timmer, Addressing parameter identifiability by model-based experimentation, *IET Systems Biology*, 5:120–130, 2011.

[8] Y. Gan, Q. Duan, W. Gong, C. Tong, Y. Sun, W. Chu, A. Ye, C. Miao, Z. Di, A comprehensive evaluation of various sensitivity analysis methods: A case study with a hydrological model, *Environmental Modelling and Software*, 51:269–285, 2014.

[9] R. W. Briehl, Nucleation, fiber growth and melting, domain formation and structure in sickle hemoglobin gels, *Journal of Molecular Biology*, 245:710–723, 1995.

[10] N. Daniel-Jones, M. Chen, D. P. Clemence, G. Gibson, A mathematical model for the sickle cell depolymerization dynamical properties and numerical experiments, *International Journal of Qualitative Theory of Differential Equations and Applications*, 2:183-200, 2008.

[11] J. A. David, *Optimal Control, Estimation, and Shape Design: Analysis and Applications*, PhD Dissertation, North Carolina State University, USA, 2007.

[12] H. T. Banks, S. Dediu, S. L. Ernstberger, F. Kappel, Generalized sensitivities and optimal experimental design, *Journal of Inverse and Ill-posed Problems*, 18:25–83, 2010.

[13] G. M. Hornberger, R. C. Spear, An approach to the preliminary analysis of environmental systems, *Journal of Environmental Management*, 12:7–18, 1981.

[14] F.-J. Chang, J. W. Delleur, Systematic parameter estimation of watershed acidification model, *Hydrology Processes*, 6:29–44, 1992.

[15] J. Choi, S. M. Hulseapple, M. H. Conklin, J. W. Harvery, Modeling CO_2 degassing and pH in a stream-aquifer system, *Journal of Hydrology*, 209:297–310, 1998.

[16] K.-H. Cho, S.-Y. Shin, W. Kolch, O. Wolkenhauer, Experimental design in systems biology, based on parameter sensitivity analysis using a Monte Carlo method: a case study for the TNF α-mediated $NF-\kappa B$ signal transduction pathway, *Simulation*, 79:726–739, 2003.

[17] R. Alves, M. A. Savageau, Systemic properties of ensembles of metabolic networks: application of graphical and statistical methods to simple unbranched pathways, *Bioinformatics*, 16:534–547, 2000.

[18] Z. Zi, K. H. Cho, M. H. Sung, X. Xia, J. Zheng, Z. Sun, In silico identification of the key components and steps in IFN-γ induced JAK-STAT signaling pathway, *FEBS Letters*, 597:1101–1108, 2005.

[19] P. E. Keipert & MP4CO-SCD-105 Study Investigators, Clinical evaluation of MP4CO: A phase 1b escalating-dose, safety and tolerability study in stable adult patients with sickle cell disease, *Oxygen Transport to Tissue XXXVIII*, Advances in Experimental Medicine and Biology, 923, Springer, Cham, 2016.

[20] J. G. Louderback, S. Kh. Aroutiounian, W. C. Kerr, S. K. Ballas, D. B. Kim-Shapiro, Temperature and domain size dependence of sickle cell hemoglobin polymer melting in high concentration phosphate buffer, *Biophysical Chemistry*, 80:21–30, 1999.